**Proceedings of the Utah NASA Space Grant Consortium &
Annual Fellowship Symposium
UNSGC 2019
May 6, 2019, Provo, USA**

DJB2019

BOILING HEAT TRANSFER OF IMPINGING JETS ON SUPERHEATED SUPERHYDROPHOBIC SURFACES

D. Jacob Butterfield*, Julie Crockett
Fluids and Thermal Transport Laboratory
Department of Mechanical Engineering
Brigham Young University
Provo, Utah 84602

ABSTRACT

Superhydrophobic surfaces possess desirable self-cleaning properties, but have also been shown to reduce heat transfer to subcooled water in impinging jet scenarios. Further investigation is required to explore the potential utility of such surfaces in high temperature applications such as rocket launch-pad cooling. Here, superheated silicon substrates with varying wettability are quenched by an impinging water jet, where the substrate temperature is above the boiling regime which has previously been unexplored. Silicon wafers are etched, coated, and integrated with an electric resistance heater and heated to temperatures up to 300 ° C before being quenched by an axisymmetric water jet. The early results of this study confirm previous conjecture that decreased surface wettability is correlated to decreased heat transfer for the described scenario.

*Address all correspondence to this author at dbutter2@byu.edu.

NOMENCLATURE

a	jet radius
c_p	specific heat
h	heat transfer coefficient
k	thermal conductivity
m	meters
mm	millimeters
Q	volume flow rate
q”	heat flux
r	radial distance from stagnation point
Re	jet Reynolds number
t	time
T_j	jet temperature
T_s	local surface temperature
v	velocity
W	Watts

Greek Symbols

δ	wafer thickness
ρ	density

Subscripts

si	Silicon
w	Water
H	Heater

INTRODUCTION

Liquid jet impingement is utilized in many cooling applications due to the ability of the fast-moving, high-convection thin films that are formed to provide significant heat transfer from a surface [1]. This method of heat transfer already finds application in metal processing [2], piston cooling (with oil as the working fluid) [3], gas turbine cooling [4], and emergency nuclear reactor cooling [5]. There are also important applications for jet impingement that further the interests of NASA, including better electronics cooling for mission controls, rapid rocket launchpad cooling, and rocket nozzle or jet turbine cooling. One common issue in many of these industrial applications is that the ability to transfer heat is reduced by fouling that can occur due to dust and debris accumulation on the heated surface [6]. Operations are interrupted in order to clean these surfaces, which further inhibits production or performance.

Superhydrophobic (SH) surfaces are a potential solution for the issue of fouling. Water-repelling SH surfaces are manufactured by altering surface geometry to provide micro- or nano-scale roughness as shown in Figure 1, left image, and by changing the surface chemistry to make it inherently hydrophobic due to low surface energy. This combination of surface modification alters the adhesive force of water molecules on the surface, as they have contact only on the highest points of the rough surface and air gaps are left beneath, which causes droplets to bead up. SH surfaces are defined as having a liquid-solid contact angle of 150 °C or more (see Figure 1, right image). Surfaces with such low adhesion to water provide high droplet mobility, which results in the desirable self-cleaning property for jet impingement heat transfer applications.

Only a few prior works on the use of SH surfaces in jet impingement have been accomplished, with an emphasis on hydrodynamics [7, 8]. The research I am conducting investigates the usefulness of SH surface implementation in jet impingement heat transfer situations at superheated wall temperatures.

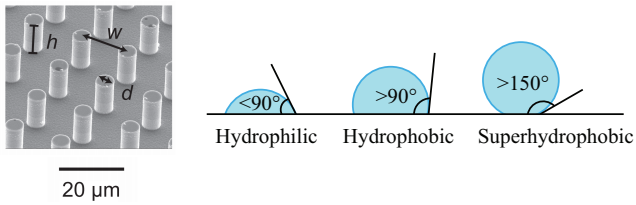

FIGURE 1: SEM image of post microstructures (left, from [8]). Level of hydrophobicity is defined by the contact angle at the triple contact line of a water droplet on a surface (right, from [9]).

To provide a visual on jet impingement, Figure 2 shows a radial cross-section of an impinging jet showing the following defined regions of impingement:

I. *Stagnation region*: Characterized by high pressure and acceleration in the radial direction, and consequently high heat transfer coefficient.
II. *Thin film region*: Water spreads out and flows across the surface, also known as the parallel-flow region for planar jets or the radial-flow region for axisymmetric jets.
III. *Downstream depth region with hydraulic jump*: At a certain critical distance from the stagnation region, the hydrostatic forces and surface tension balance with momentum and form a hydraulic jump. Downstream the fluid velocity slows and the liquid height increases considerably.

Research exploring jet impingement, which will be summarized in the succeeding paragraphs to demonstrate the underlying physics behind my research. The first in-depth study performed on the hydrodynamics of impinging liquid jets, which was by Watson in 1964 [10]. Watson characterized the flow of an impinging jet and produced fairly accurate predictive equations for the radial location of the hydraulic

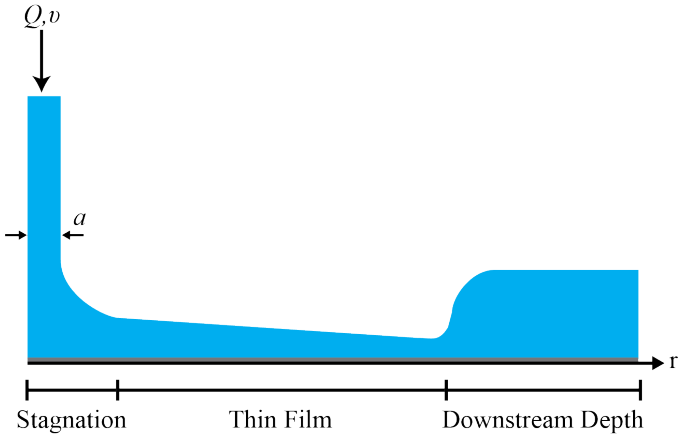

FIGURE 2: Radial cross-section view of an impinging jet, divided as follows: I - Stagnation region, II - Thin film region, III - Downstream depth region with hydraulic jump.

jump. At this jump the hydrostatic pressure and surface tension overcome the momentum. The result can be seen in Figure 2 as an increase in liquid depth and decrease in fluid speed. A more thorough investigation was performed by Liu and Lienhard, who researched the flows and eddies produced by impinging jets [11]. Other research includes Lienhard's contribution on the effect of nozzle type and jet velocity [1], and the contribution of Bush *et al.* which added surface tension to Watson's model [12, 13]. Thus, a foundation for the fluid dynamics of impinging jets has previously been laid.

Heat transfer properties of impinging jets in single-phase convection [14–17] and nucleate boiling (vapor bubbles generated at the heated surface) [18–22] have been heavily investigated, showing that heat transfer improves drastically as the nucleate boiling condition is reached. These authors have explored the impacts on heat transfer of jet subcooling, wall temperature, jet length (nozzle-to-surface spacing), spatial variation in the radial direction, and laminar versus turbulent jets. Other researchers [2, 23–27] have studied transition and film boiling in jet impingement and created mathematical models for various spatial regions of the impinging jet. However, boiling heat transfer has never been researched in connection with SH surfaces.

In addition to the extensive research on steady-state jet impingement boiling, there have also been several studies investigating the transient effects of quenching superheated metal surfaces [28–33]. Several experimental techniques were utilized in order to acquire the time-sensitive data readings necessary for heat transfer calculations, including the use of thermocouples or balancing the heat removed with the supplied heat.

Some research has investigated the hydrodynamics of impinging jets on SH surfaces. The published results have shown that the radial flow following the thin film region tends to break up into droplets rather than reach a hydraulic jump unless a downstream depth is imposed [7, 34]. The effects of inclined jets rebounding on SH surfaces has also explored [35]. Little has been examined, however, regarding the effects of SH properties on the effectiveness of jet impingement heat transfer [8].

One important conclusion from the sparse research performed regarding heat transfer on SH surfaces demonstrated that the air gaps act as an insulating layer to heat transfer. It is expected that there will be little or no nucleate boiling on the SH surfaces [36]. Rather, less effective film boiling (vapor bubbles are generated so rapidly that a film of vapor is formed under the liquid layer) is anticipated to occur based off quenching research done by Vakarelski *et al.* [37]. Interestingly, research done by Qiu and Liu on *superhydrophilic* surfaces reported heat fluxes 30% higher on surfaces with low contact angle [38], so it is likely that lower heat fluxes would be observed on SH surfaces. Searle *et al.* [8] created models predicting the local Nusselt number for various spatial regions along the surface for sub-critically heated surfaces with jet impingement and found that as cavity fraction (ratio of etched microfeature surface area to total surface area) increased on the surface, lower heat transfer was observed. However, this work only dealt with single-phase forced convection heat transfer, which is not the primary mode of heat transfer for supercritical temperatures.

The potential trade-offs remain to be clarified between the desirable self-cleaning properties of SH surfaces and the reduced heat transfer effectiveness of film boiling. It is imperative that experimental tests be performed comparing two-phase heat transfer from an impinging jet on superheated SH surfaces to superheated hydrophilic and smooth hydrophobic surfaces (no geometry alteration) in order to better demonstrate these trade-offs.

METHODS

The experimental apparatus and method used to collect data was similar to that of Searle *et al.* [39]. Significant differences arise, however, as a transient study was performed involving much higher surface temperatures. This section will cover the experimental apparatus, data acquisition, and data analysis techniques used in this study.

Experimental Apparatus

There are three main components that comprise experimental apparatus: the surfaces, the jet and associated hardware, and the cameras. A schematic of the apparatus is shown in Figure3. For the standard case, a blank silicon wafer with diameter of 100 mm and thickness 525 μm was screen-printed with a silver paste on the backside to create an integrated electrical resistance heater. The heater was designed with a nominal diameter of 51 mm, providing 0.25 Ω of resistance. Leads were attached to the heater connecting it to a 20-V, 120-A DC power supply. The heaters were spray-painted with a flat black coating of known emissivity for accuracy and ease of thermal reading.

Hydrophobic surfaces were created by modifying the previous method slightly. After screen-printing and before adding the wire leads, the wafers had a thin layer (100 nm) of chromium deposited via electron-beam evaporation followed by a thin layer (200 nm) of natively hydrophobic DuPont™ Teflon® (commercial brand of polytetrafluoroethylene, PTFE) that was spin-coated onto the surface. This resulted in static water contact angles of 120° as measured by an electronic goniometer code implemented in MATLAB.

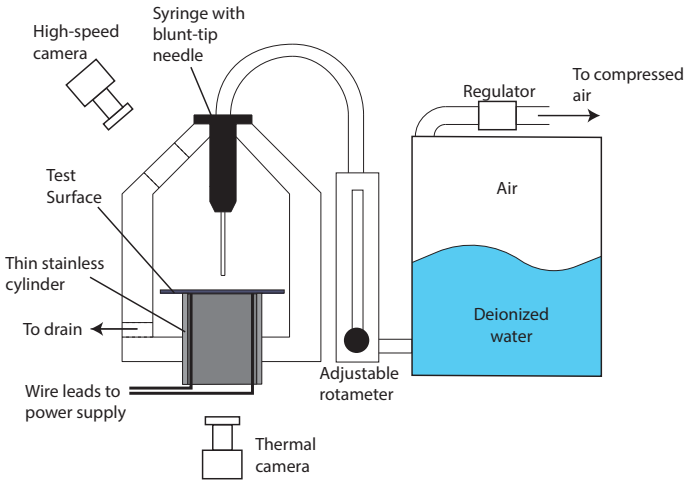

FIGURE 3: Schematic of experimental apparatus.

SH surfaces were fabricated by first patterning the silicon wafers using standard photolithography methods. They were then etched using a reactive ion etching (RIE) process that created microscale posts of pitch 16 μm and depth 24 μm (see Fig. 1). The procedure was then the same for applying a hydrophobic coating and the integrating heating units. SH surfaces that were fabricated for this study had static contact angle measurements of 160°.

The jet subsystem consists of a long (15 cm) stainless steel nozzle of inner radius r_j = 1.275 mm connected to a rotameter. The rotameter is attached to a pressure tank containing pure water. Compressed air is introduced to the tank, pushing on a diaphragm that creates the driving pressure for the jet flow. The nozzle is situated nominally 2 in. above the wafer to be tested, which itself is seated on a large stainless steel cylinder which inhibits conduction from the wafer due to its relatively low thermal conductivity, thin upper walls, and large thermal mass. The water empties from the edges of the wafer into a 3D-printed plastic collection container that also supports the entire subsystem.

The stainless steel cylinder is hollowed in the center to allow access to a FLIR thermal camera, which

records data from below at a frame rate of nominally 200 Hz and a resolution of 320 x 256 pixels. High-speed data is also taken by a Photron Fastcam APX RS located above the wafer at an angle. The high-speed images were taken at a frame rate of 500 Hz and a spatial resolution of 1024 x 1024 pixels.

Data Acquisition

Data was taken by synchronizing sequences of images via an electronic trigger activated just as impingement begins. The surface was electrically heated until the maximum surface temperature reached the prescribed value of 280°C, after which the rotameter was opened and the camera trigger enabled. Spatial calibration images are taken before any data recording to provide the correct conversion from pixels to mm, and an unheated scenario provides the water temperature that is used in calculating the heat transfer coefficient.

Data Analysis

Data taken from the thermal and high-speed cameras is analyzed in a MATLAB script, which calculates the heat flux from the silicon wafer to the jet as a function of radius and time. This is done by averaging the temperature field data over twenty equally-spaced radial lines and then numerically solving the energy balance:

$$q"(r,t) = k_{si}\delta\frac{\partial^2 T}{\partial r^2} + \frac{1}{r}\frac{\partial T}{\partial r} + \frac{q_H}{\pi r_H^2} - \rho\delta c_p\frac{\partial T}{\partial t} \quad (1)$$

where $q"$ is the heat flux to the jet as a function of radial position, r, and time, t; k_{si}, ρ, and c_p are the thermal conductivity, density, and specific heat of silicon, respectively; δ is the wafer thickness; q_H represents the heater input; T is the temperature field. Eqn. 1 accounts for the heater input, conjugate heat transfer in the radial direction, and the time-resolved storage term. The wafer itself is treated as uniform temperature along its thickness.

After obtaining the heat flux data, the process of obtaining the overall non-dimensional heat transfer

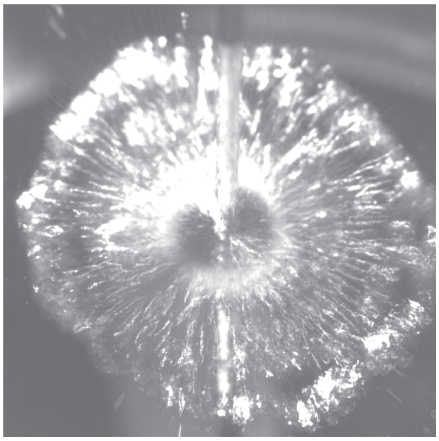

(a) High-speed data

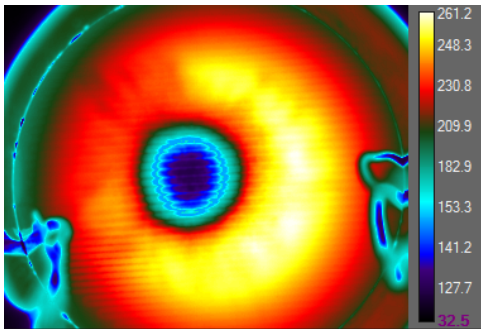

(b) Thermal data

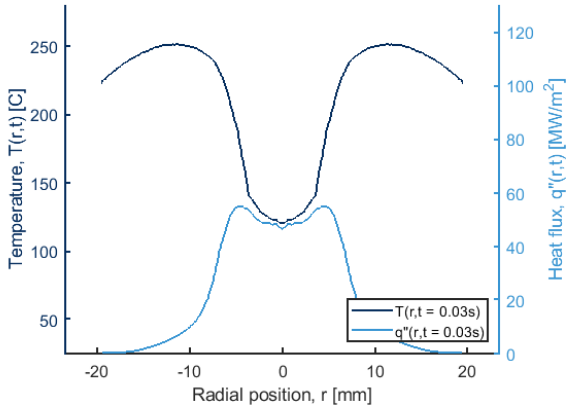

(c) Analyzed heat flux data

FIGURE 4: Jet impingement cooling for a smooth hydrophobic surface at t = 0.03 s. Temperature and heat flux data are correlated spatially to the high-speed and thermal images.

coefficient $Nu = h\delta/k_{si}$ is simply a solution of Newton's law of cooling, normalized by the jet radius and liquid thermal conductivity. The comparison of Nu for different surface wettability can be a key indicator of the jet impingement boiling heat transfer capability, but is not included in this report as it is very similar to the heat flux data.

RESULTS

Typical analysis images are show in Figure 4 where analyzed heat flux data is aligned with the high-speed and thermal data for a smooth hydrophobic surface at a time of t = 0.03 s after impingement. The stagnation point is selected from the thermal data where it is at a global minimum and 20 lines are averaged radially outward, with the electrical wire temperatures being neglected at the edges. This averaging spatially constitutes the temperature profile found in the plot, and the heat flux, shown in correlation to the right axis, is calculated based on the solution to the described energy balance for each radial location at every instance in time.

Some important features to note from these visuals include the constant surface heat flux condition provided by the integrated heater, as initially there is not a uniform temperature across the surface. Another interesting artifact apparent in the high-speed data is that there is a visible region at the stagnation point where boiling has ceased and convection has begun. Beyond that region there is a ring where boiling occurs. Surrounding that boiling region, water droplets are ejected and spread out, hovering above the surface but not contributing to its cooling. Here, the synchronization of the data is critical because the temperature profile shows the higher temperatures that are more constant in time towards the edges, and the cooling effect of the jet has not affected those regions yet despite the presence of satellite droplets above the surface.

The images in Figure 5 compare spatial temperature distribution and heat flux to the cooling jet at different instances of time for both hydrophilic (HPi) as well as smooth hydrophobic (HPo) surfaces. It can be noticed that the highest heat flux occurs at early times, when the temperature difference is greatest. As time increases, the maximum heat flux travels radially outward along the so-called wetting front, where boiling behavior is still occurring and has not transitioned to convection cooling. This is evidenced again by the correlation of radial heat flux profile to the high-speed images.

Temperatures in Figure 5 range from a starting maximum of 280°C, and by 0.1 s after impingement have already dropped to a minimum of around 50°C. This demonstrates clearly the potential of an impinging jet for heat transfer. The high outer peaks of the temperature profile as the center is cooled makes conjugate heat transfer within the wafer very apparent as there is nearly the same temperature difference throughout the wafer as the initial difference between surface and jet temperatures.

As t increases, the maximum surface heat flux becomes more similar for both cases, emphasized by the case of t = 0.1 s where the heat flux peaks at around $30\ W/m^2$. The temperature profiles also approach one another as convective heat transfer begins dominating the majority of the wafer surface and its temperature approaches that of the impinging jet.

DISCUSSION

As is seen from the results of the work performed thus far, hydrophilic surfaces have the capacity to cool surfaces faster and have maximum heat fluxes that are higher by up to 33%, especially at the initial cooling stages. The temperature also decreases more rapidly, as was anticipated due to the preferred wetting state. At just 0.02 s after impingement, the hydrophilic surface already demonstrates a minimum temperature of 50°C less than the hydrophobic case.

Work is ongoing for work with SH surfaces, which will have even less direct contact with the impinging jet and should further decrease heat transfer. Based off the results in this report, the decrease should be much more significant as the cavity fraction (the ratio of space between contact points to the total projected

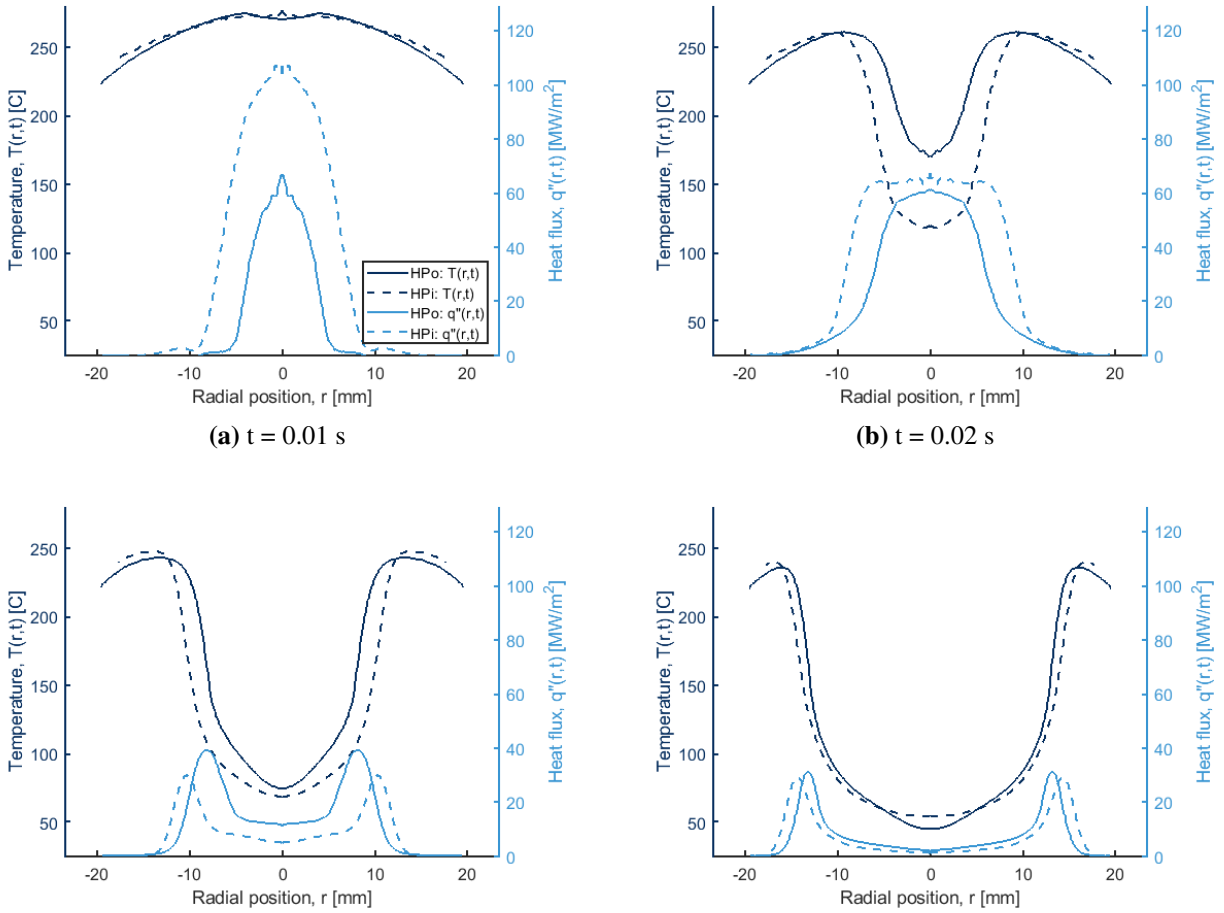

(a) t = 0.01 s

(b) t = 0.02 s

(c) t = 0.05 s

(d) t = 0.1 s

FIGURE 5: Impingement cooling progression for multiple times. Results of both temperature and heat flux as functions of surface wettability, time, and location are shown.

surface area) will contribute to the insulation of the wafer from water contact.

As different surface geometries are investigated in future work, other factors will also be tested for their influence. Some of these will include nozzle diameter, jet flow rate, and angle of impingement. The techniques employed here provide a broad range of data, from quantitative temperature and heat flux measurements to qualitative images that show the actual jet behavior at the surface. This will be useful in the next phase of research as models can be created that can be used predictably for use in applications previously mentioned.

ACKNOWLEDGMENT

Funding for this research has been supported by the National Science Foundation [grant number: CBET-1707123] and by the Utah NASA Space Grant Consortium.

REFERENCES

[1] Lienhard, J. H., 1995. "Liquid Jet Impingement". *Annual Review of Heat Transfer,* ***6***(6), pp. 199–270.

[2] Filipovic, J., Incropera, F. P., and Viskanta, R., 1995. "Quenching Phenomena Associated with a Water Wall Jet: II. Comparison of Experimen-

tal and Theoretical Results for the Film Boiling Region". *Experimental Heat Transfer,* ***8***(2), pp. 119–130.

[3] Nasif, G., Barron, R., and R., B., 2015. "The Application of Jet Impingement for Piston Cooling". In 11th International Conference on Heat Transfer, Fluid Mechanics and Thermodynamics, pp. 481–486.

[4] Han, B., and Goldstein, R. J., 2001. "Jet-Impingement Heat Transfer in Gas Turbine Systems". *Annals Of The New York Academy Of Sciences,* ***934***, pp. 147–161.

[5] Mitsutake, Y., and Monde, M., 2001. "Heat transfer during transient cooling of high temperature surface with an impinging jet". *Heat and Mass Transfer/Waerme- und Stoffuebertragung,* ***37***(4-5), pp. 321–328.

[6] Awad, M. M., 2011. "Fouling of heat transfer surfaces". In *Heat Transfer - Theoretical Analysis, Experimental Investigations and Industrial Systems*, A. Belmiloudi, ed. InTech, ch. 20, pp. 505–542.

[7] Prince, J. F., Maynes, D., and Crockett, J., 2015. "On jet impingement and thin film breakup on a horizontal superhydrophobic surface". *Physics of Fluids,* ***27***(11).

[8] Searle, M., Maynes, D., and Crockett, J., 2017. "Thermal transport due to liquid jet impingement on superhydrophobic surfaces with isotropic slip". *International Journal of Heat and Mass Transfer*, pp. 680–691.

[9] Stevens, K. A., Crockett, J., Maynes, D. R., and Iverson, B. D., 2017. "Two-phase flow pressure drop in superhydrophobic channels". *International Journal of Heat and Mass Transfer,* ***110***, jul, pp. 515–522.

[10] Watson, E. J., 1964. "The radial spread of a liquid jet over a horizontal plane". *Journal of Fluid Mechanics,* ***20***(3), pp. 481–499.

[11] Liu, X., and Lienhard V, J. H., 1993. "The hydraulic jump in circular jet impingement and in other thin liquid films". *Experiments in Fluids,* ***15***(2), pp. 108–116.

[12] Bush, J. W. M., and Aristoff, J. M., 2003. "The influence of surface tension on the circular hydraulic jump". *Journal of Fluid Mechanics,* ***489***(489), pp. 229–238.

[13] Bush, J. W. M., Aristoff, J. M., and Hosoi, A. E., 2006. "An experimental investigation of the stability of the circular hydraulic jump". *Journal of Fluid Mechanics,* ***558***, p. 33.

[14] Webb, B., and Ma, C.-F., 1995. "Single-Phase Liquid Jet Impingement Heat Transfer". *Advances in Heat Transfer,* ***26***, pp. 105–217.

[15] Liu, X., and Lienhard, J. H., 1989. "Liquid jet impingement heat transfer on a uniform flux surface". *HTD,* ***106***(Heat Transfer Phenomena in Radiation, Combustion, and Fires), pp. 523–529.

[16] Liu, X., Lienhard, J. H., and Lombara, J. S., 1991. "Convective Heat Transfer by Impingement of Circular Liquid Jets". *Journal of Heat Transfer,* ***113***(3), p. 571.

[17] Elison, B., and Webb, B., 1994. "Local heat transfer to impinging liquid jets in the initially laminar, transitional, and turbulent regimes". *International Journal of Heat and Mass Transfer,* ***37***(8), pp. 1207–1216.

[18] Monde, M., and Katto, Y., 1978. "Burnout in a high heat-flux boiling system with an impinging jet". *International Journal of Heat and Mass Transfer,* ***21***(3), pp. 295–305.

[19] Monde, M., 1987. "Critical Heat Flux in Saturated Forced Convection Boiling on a Heated Disk With an Impinging Jet". *Journal of Heat Transfer,* ***109***, pp. 991–996.

[20] Kamata, C., 1999. "Experimental Study on Boiling Heat Transfer with an Impinging Jet on a Hot Block". *Heat Transfer -Asian Research,* ***28***(5), pp. 418–427.

[21] Robidou, H., Auracher, H., Gardin, P., and Lebouché, M., 2002. "Controlled cooling of a hot plate with a water jet". *Experimental Thermal and Fluid Science,* ***26***(2-4), pp. 123–129.

[22] Timm, W., Weinzierl, K., and Leipertz, A., 2003. "Heat transfer in subcooled jet impingement boiling at high wall temperatures". *Interna-*

tional Journal of Heat and Mass Transfer, ***46***(8), pp. 1385–1393.

[23] Kokado, J.-i., Hatta, N., Takuda, H., Harada, J., and Yasuhira, N., 1984. "An analysis of film boiling phenomena of subcooled water spreading radially on a hot steel plate". *Archiv für das Eisenhüttenwesen,* ***55***(3), pp. 113–118.

[24] Ma, C. F., Gan, Y. P., and Lei, D. H., 1993. "Liquid Jet Impingement Heat Transfer with or without Boiling". *Journal of Thermal Science,* ***2***(1), pp. 32–49.

[25] Liu, Z.-H., and Wang, J., 2001. "Study on film boiling heat transfer for water jet impinging on high temperature flat plate". *International Journal of Heat and Mass Transfer,* ***44***(13), pp. 2475–2481.

[26] Seiler-Marie, N., Seiler, J. M., and Simonin, O., 2004. "Transition boiling at jet impingement". *International Journal of Heat and Mass Transfer,* ***47***(23), pp. 5059–5070.

[27] Nobari, A. H., Prodanovic, V., and Militzer, M., 2016. "Heat transfer of a stationary steel plate during water jet impingement cooling". *International Journal of Heat and Mass Transfer,* ***101***, pp. 1138–1150.

[28] Ishigai, S., Nakanishi, S., and Ochi, T., 1978. "Boiling Heat Transfer for a Plane Water Jet Impinging on a Hot surface". In 6th International Heat Transfer Conference, pp. 445–450.

[29] Ochi, T., Nakanishi, S., Kaji, M., and Ishigai, S., 1984. *Multi-Phase Flow and Heat Transfer III. Part A: Fundamentals "Cooling of a Hot Plate with an Impinging Circular Water Jet"*. Elsevier Science Publishers B.V., Amsterdam.

[30] Hall, D. E., Incropera, F. P., and Viskanta, R., 2001. "Jet Impingement Boiling From a Circular Free-Surface Jet During Quenching: Part 1—Single-Phase Jet". *Journal of Heat Transfer,* ***123***(5), p. 911.

[31] Kumagai, S., Suzuki, S., Sano, Y., and Kawazoe, M., 1995. "Transient Cooling of a Hot Metal Plate with an Impinging Water Jet". In ASME/JSME Thermal Engineering Conference, Vol. 2, pp. 347–352.

[32] Ma, C. F., Zhao, Y. H., Yu, J., and Tian, Y. Q., 1990. "An Analytical Study of Jet Impingement Film Boiling". In First International Conference on Energy Conversion and Energy Sources Engineering, pp. 223–228.

[33] Waldeck, S., and Fritsching, U., 2017. "Heat Transfer in the Boiling Regime of Impinging Liquid Jets". In 2nd World Congress on Momentum, Heat and Mass Transfer.

[34] Maynes, D., Johnson, M., and Webb, B. W., 2011. "Free-surface liquid jet impingement on rib patterned superhydrophobic surfaces". *Physics of Fluids,* ***23***(5).

[35] Kibar, A., 2016. "Experimental and numerical investigations of the impingement of an oblique liquid jet onto a superhydrophobic surface: energy transformation". *Fluid Dynamics Research,* ***48***(1), p. 015501.

[36] Clavijo, C. E., Crockett, J., and Maynes, D., 2017. "Hydrodynamics of droplet impingement on hot surfaces of varying wettability". *International Journal of Heat and Mass Transfer,* ***108***, pp. 1714–1726.

[37] Vakarelski, I. U., Patankar, N. A., Marston, J. O., Chan, D. Y., and Thoroddsen, S. T., 2012. "Stabilization of Leidenfrost vapour layer by textured superhydrophobic surfaces". *Nature,* ***489***(7415), pp. 274–277.

[38] hao Qiu, Y., and hua Liu, Z., 2008. "Nucleate boiling on the superhydrophilic surface with a small water impingement jet". *International Journal of Heat and Mass Transfer,* ***51***(7-8), pp. 1683–1690.

[39] Searle, M. C., Crockett, J., Jensen, B. D., Iverson, B. D., Jones, M. R., and Searle, M. C., 2018. "Thermal Transport at Superhydrophobic Surfaces in Impinging Liquid Jets, Natural Convection, and Pool Boiling". PhD thesis, Brigham Young University.